Applied Clay Science 132–133 (2016) 412–418

Contents lists available at ScienceDirect

Applied Clay Science

journal homepage: www.elsevier.com/locate/clay

Research paper

Adsorption of polyhydroxy fullerene on polyethylenimine-modified montmorillonite

Qingze Chen [a,b], Runliang Zhu [a,*], Yanping Zhu [a,b], Jing Liu [a,b], Lifang Zhu [c], Lingya Ma [a,b], Meng Chen [a]

[a] CAS Key Laboratory of Mineralogy and Metallogeny, Guangdong Provincial Key Laboratory of Mineral Physics and Material Research & Development, Guangzhou Institute of Geochemistry, Chinese Academy of Sciences, Guangzhou 510640, China
[b] University of Chinese Academy of Sciences, Beijing 100049, China
[c] Zhejiang University of Water Resources and Electric Power, Hangzhou 310018, China

ARTICLE INFO

Article history:
Received 17 March 2016
Received in revised form 9 July 2016
Accepted 11 July 2016
Available online 18 July 2016

Keywords:
Polyhydroxy fullerene
Polyethylenimine
Montmorillonite
Adsorption

ABSTRACT

The environmental behaviors and potential ecotoxicity of carbon nanomaterials, such as fullerene and its derivatives, are gaining ever-increasing concerns at present. This work attempts to develop an adsorbent for the effective removal of polyhydroxy fullerene (PHF) from aqueous solution, which was synthesized by modifying montmorillonite (Mt) with a branched polymer polyethylenimine (PEI). The adsorption results showed that the obtained adsorbent (*i.e.*, PEI-Mt) could effectively remove PHF over a wide range of solution pH; both the electrostatic attraction and hydrogen-bond interaction between PHF and PEI-Mt contributed to the strong adsorption. Decreasing solution pH and rising PEI loading amount on Mt could both increase the adsorption amounts of PHF on PEI-Mt. The adsorption isotherms could be well fitted with the Langmuir model, and the calculated maximum adsorption value of PHF on 10%PEI-Mt reached ~213 mg/g, much higher than that on the original Mt (~16 mg/g). The adsorbents after PHF adsorption were further characterized using Fourier transform infrared spectroscopy, X-ray diffraction, and transmission electron microscopy. The results suggested that the adsorbed PHF primarily existed on the outer surfaces of PEI-Mt. This work showed that PEI-Mt can be a potentially efficient adsorbent for the removal of PHF from aqueous solution.

1. Introduction

Fullerene and its derivatives have gained immense attention so far due to their remarkable properties and potential applications in many areas, including environmental remediation (*e.g.*, adsorbents and catalysts) (Yang et al., 2006; Meng et al., 2012), biomedicine (*e.g.*, antibacterial and antitumor) (Markovic and Trajkovic, 2008; Kwag et al., 2013), and materials science (*e.g.*, sensors, supercapacitors, and hydrogen storage) (Li et al., 2009; Xiong et al., 2012; Rather and De Wael, 2013). With the ever-increasing production and wide applications of fullerene-based carbon nanomaterials, they will inevitably enter into the environment (Colvin, 2003; Klaine et al., 2008). As such, significant concerns have been drawn to their influences on human health and natural environment.

Although fullerene is highly hydrophobic, water-soluble fullerenes, such as aqueous fullerene colloid aggregates (nC_{60}) and polyhydroxy fullerene (PHF), can be conveniently synthesized by ultrasonication, solvent exchange, and chemical modification (Brant et al., 2006; Georgieva et al., 2013). The enhanced water-solubility expands their applications, but may simultaneously increase their risks to the environment and human health (Klaine et al., 2008). Indeed, the cytotoxicity of water-soluble fullerenes to both bacteria and human cell has been confirmed by many studies (Sayes et al., 2004; Wielgus et al., 2010; An and Jin, 2012). Consequently, proactive research on effective removal of water-soluble fullerenes from aqueous solution is critical to controlling the potential risks and ensuring a sustainable carbon nanomaterials industry.

At present, a number of studies have been conducted to remove nC_{60} from wastewater by various adsorbents, such as biomass (Kiser et al., 2010), activated sludge (Yang et al., 2013), and alum (Wang et al., 2013). In contrast, much less work about the pollution control of PHF has been reported up to now. On the other hand, Prylutskyy et al. (2014) indicated that the origin of fullerene solubility in water was probably based on the surface hydroxylation of fullerene molecules; therefore, nC_{60} could be considered as fullerene aggregates with a certain amount of hydroxyls on the outer surfaces. Furthermore, when exposed to the environment, fullerenes and nC_{60} could be transformed into PHF by many factors (*e.g.*, long-term mixing, ultraviolet radiation, and interaction with microbes and oxidants) (Hwang and Li, 2010; Qu et al., 2010; Chae et al., 2014). Hence, being regarded as the main products of fullerenes in the environment, PHF need large concerns in terms of their pollution control.

* Corresponding author.
E-mail address: zhurl@gig.ac.cn (R. Zhu).

http://dx.doi.org/10.1016/j.clay.2016.07.007
0169-1317/

Table 1
Meanings of the abbreviations for the samples.

Abbreviation	Meaning
PHF	Polyhydroxy fullerene
PEI	Polyethylenimine
Mt	Montmorillonite
2%PEI-Mt	2%PEI-modified Mt
10%PEI-Mt	10%PEI-modified Mt
Mt-PHF	Mt after the adsorption of PHF (C_0 = 400 mg/L)
2%PEI-Mt-PHF	2%PEI-Mt after the adsorption of PHF (C_0 = 400 mg/L)
10%PEI-Mt-PHF	10%PEI-Mt after the adsorption of PHF (C_0 = 400 mg/L)

With 2D nano-sized structure, high cation exchange capacity, and large specific surface area, montmorillonite (Mt) as a low-cost and environmental-friendly adsorbent for cationic contaminants (*e.g.*, cationic dyes and heavy metal cations) has been widely applied in environmental remediation (Bergaya and Lagaly, 2013; Yuan et al., 2013; Zhu et al., 2016). However, owing to the negatively charged layers, raw Mt exhibits a poor affinity toward anionic contaminants (Zhu et al., 2016). A number of studies indicated that Mt could be easily modified by cationic modifiers to synthesize various adsorbents, such as the cationic surfactant modified Mt for organic contaminants (Roberts et al., 2006; Zhu et al., 2011), and the hydroxymetal polycations modified Mt for oxyanions (Zhou et al., 2010; Ma et al., 2015). As an important type of modifiers for Mt, the cationic polymers have received broad attentions because of their large charge/mass ratio (Yue et al., 2007; Zhu et al., 2010). In this regard, cationic polymers could readily saturate the CEC of Mt and change the surface charge of Mt from negative into positive. As a result, the modified Mt could provide adsorption sites for anionic contaminants (Kang et al., 2009; Li et al., 2011). Given that PHF generally exhibit negative surface charges in water (Brant et al., 2007), one could propose that cationic polymers-modified Mt may be an efficient adsorbent for PHF.

Herein, polyethylenimine (PEI), a water-soluble cationic polymer with a large number of amino groups and high charge density (Fig. S1) (Zhang et al., 2014), was selected to modify Mt. The adsorption capacities of Mt and the PEI-modified Mt (PEI-Mt) toward PHF were investigated, and the potential adsorption mechanisms were further elucidated through X-ray diffraction (XRD), transmission electron microscopy (TEM), and Fourier transform infrared spectroscopy (FTIR). Our results indicated that PEI-Mt exhibited high affinity toward PHF, with the maximum adsorption amount of ~213 mg/g. As such, PEI-Mt could be used as a promising adsorbent toward PHF.

2. Materials and methods

2.1. Materials

The sodium-exchanged Mt used in this work was prepared by dispersing the calcium-rich Mt (CEC was 110.5 mmol/100 g, purity >95%, Inner Mongolia, China) in a 0.5 mol/L solution of NaCl, followed by stirring for 24 h at 80 °C (repeated 3 times). The obtained suspension was centrifuged and washed repeatedly with distilled water until $AgNO_3$ test confirmed no chloride in the supernatant. After being dried at 60 °C, the sodium-exchanged Mt was collected for the follow-up experiments. For brevity, Mt was used to denote the sodium-exchanged Mt in the following text. The cationic polymer, branched PEI (molecular mass = 10,000, 99%), was supplied by Shanghai Aladdin Bio-Chem Technology Co., Ltd. PHF was purchased from Suzhou Dade Carbon Nanotechnology Co., Ltd.

2.2. Synthesis of adsorbents

PEI-Mt was prepared as follows: a desired amount of PEI was dissolved into distilled water under stirring for 10 min, followed by adding 10 g of Mt. The mixture was vigorously stirred for 12 h at room temperature, and then the resulting OMts were collected by centrifugation, washed with distilled water (3 times), and freeze-dried for 24 h. The added amounts of PEI were 2% and 10% of the weight of Mt, and the corresponding OMts were denoted as 2%PEI-Mt and 10%PEI-Mt, respectively. For clarity, the meanings of all the abbreviations for the samples are listed in Table 1.

2.3. Adsorption experiments

In order to determine the adsorption equilibration time, the adsorption kinetics experiments were conducted with the adsorption time ranged from 10 min to 24 h. In detail, 0.1 g of the adsorbents (*i.e.*, Mt and 2%PEI-Mt) were added into 20 mL of the PHF solution with the concentration of 200 mg/L. The suspension were steadily agitated in an incubator shaker at 200 rpm and 25 °C. Subsequently, the influences of pH on the adsorption of PHF on PEI-Mt were investigated. In this case, the pH was initially adjusted using 0.1 M NaOH or 0.1 M HCl, and the initial concentration of PHF for 2%PEI-Mt and 10%PEI-Mt were 200 and 800 mg/L, respectively. Besides, batch adsorption experiments were conducted to evaluate the adsorption capacities of the raw Mt and PEI-Mt toward PHF from aqueous solutions. Specifically, 0.1 g of the adsorbents were mixed with 20 mL of PHF solutions containing different

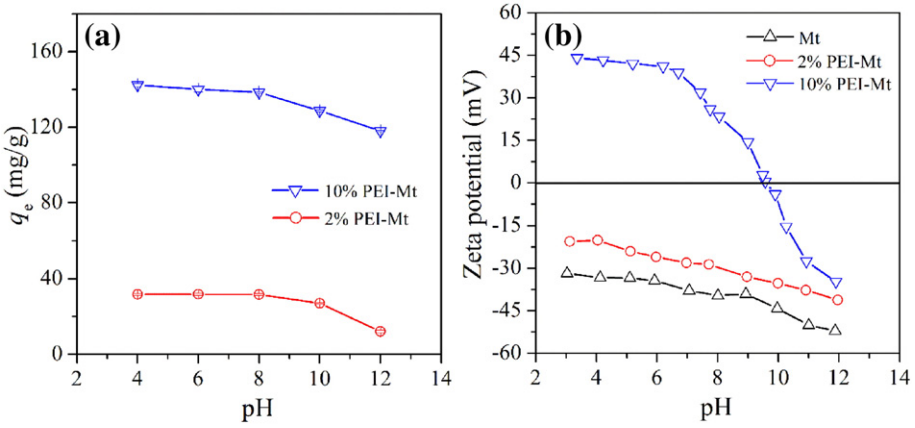

Fig. 1. Effects of pH on the adsorption capacities of 2%PEI-Mt and 10%PEI-Mt toward PHF(a). Zeta potential of Mt, 2%PEI-Mt, and 10%PEI-Mt as a function of solution pH(b).

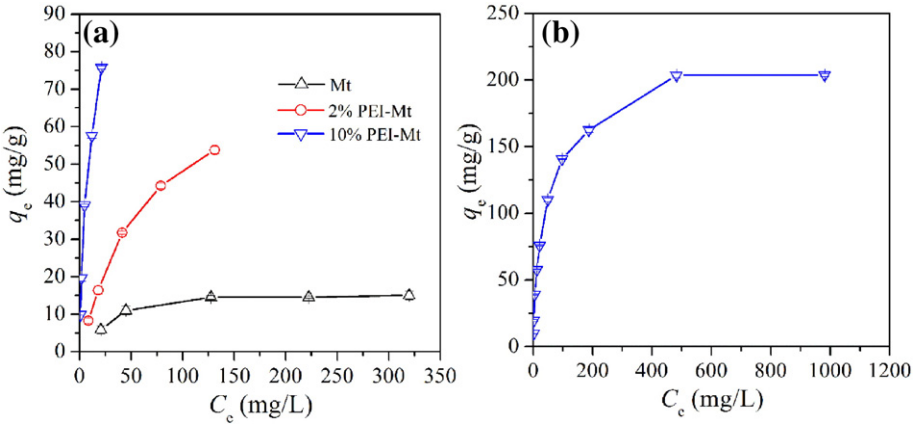

Fig. 2. Equilibrium isotherms for PHF adsorption on Mt, 2%PEI-Mt and 10%PEI-Mt (C0 = 50–400 mg/L) (a). Equilibrium isotherm for PHF adsorption on 10%PEI-Mt (C0 = 50–2000 mg/L) (b).

concentrations in a 50 mL polypropylene centrifuge tube (the initial pH = 6). Those tubes were continuously shaken in an incubator shaker at 200 rpm and 25 °C for 24 h (according to the adsorption kinetics results), and then centrifuged at 4000 rpm for 10 min to separate the products. Over the whole experiments, the concentrations of PHF in the supernatants were analyzed using the total organic carbon (TOC) analyzer (Elementar vario TOC, German). In addition, the PHF removal efficiency from aqueous solution by PEI in the absence of Mt was also investigated under the same experiment conditions as a control experiment. All the adsorption experiments were performed in duplicate.

2.4. Characterization methods

Zeta potentials measurements were performed using a nano ZS/Mastersizer 2000E instrument (Malvern Instruments Ltd., UK). The analysis pH of the suspension was adjusted with 0.1 M NaOH or 0.1 M HCl. All data were determined 5 times in each pH, and the average value was plotted to analyze the isoelectric point of the sample. The XRD patterns of the samples were determined on a Bruker D8 Advance X-ray diffractometer with Cu Kα radiation (λ = 0.154 nm) and a Ni filter, operating at 40 mA and 40 kV. The patterns were collected over the range of 3–15° at a scanning speed of 2°min^{-1}. FTIR spectra of the samples were carried out on a Brucker Vertex-70 FTIR spectrophotometer using pressed KBr disks (a mixture of 0.9 mg powdered sample and 80 mg KBr). The spectra were recorded between 4000 and 400 cm^{-1} with a resolution of 4.0 cm^{-1} and 64 scans. TEM images were characterized by a Tecnai G2 Spirit transmission electron microscope (FEI Co., USA) with the accelerating voltage of 120 kV. The samples for TEM observation were prepared as follows: 0.5 mL of the homogeneous suspension after the adsorption of PHF with the concentration of 400 mg/L (before centrifugal separation) were added in 5 mL distilled water and ultrasonically dispersed for 5 min, followed by dropping 0.1 mL of the as-prepared suspension onto the surface of a carbon-coated copper grid and air-dried before measurement. The samples for TEM observation were denoted as Mt/PHF and 10%PEI-Mt/PHF, respectively.

3. Results and discussion

The adsorption kinetics of PHF on Mt and 2%PEI-Mt were first investigated (Fig. S2). Both Mt and 2%PEI-Mt exhibited rapid adsorption rates toward PHF within the first 2 h, which could be ascribed to the abundant adsorption sites at the beginning. According to the adsorption kinetics results, the adsorption time was set at 24 h in the follow-up batch adsorption experiments.

Owing to a large number of primary and secondary amino groups on the macromolecular chains, the surface properties of PEI are highly dependent on solution pH (Amara and Kerdjoudj, 2003; Gao et al., 2009). As such, the effects of pH on the adsorption capacities of PEI-Mt toward PHF were investigated (Fig. 1a). The adsorption of PHF on both 2%PEI-Mt and 10%PEI-Mt decreased as the solution pH increased from 4 to 12. Given that about 70% of the primary and secondary amine groups in PEI molecular were protonated in acidic solution (Amara and Kerdjoudj, 2003; Gao et al., 2009), the increase in PHF adsorption could be mainly attributed to the enhanced protonation of amine groups, which could facilitate the electrostatic interaction between negatively charged PHF and positively charged amine groups in PEI molecular. Moreover, 10%PEI-Mt showed much better adsorption capacity than 2%PEI-Mt toward PHF, suggesting that increasing PEI loading amount on Mt could provide PEI-Mt more adsorption sites for PHF. This hypothesis could be further confirmed by the change in zeta potentials of the adsorbents (as shown below).

The zeta potential of Mt was affected evidently by the modification of PEI (Fig. 1b). Specifically, the isoelectric point (pH_{zpc}) of Mt could not be observed in the pH range of 3–12. The modification by PEI caused the appearance of the pHzpc of 10%PEI-Mt at pH 9.6, which could be attributed to the protonation of amine groups on the surface. Similar phenomena were reported in previous studies using PEI to modify other substances, such as silicon carbide (Zhu et al., 2003), nano-zirconia powers (Tang et al., 2000), and hematite (Chibowski et al., 2009). When the solution pH was below pH_{zpc}, the positively charged 10%PEI-Mt may effectively adsorb PHF through electrostatic interaction. Noticeably, the surface of 2%PEI-Mt was negatively-changed in the whole pH range, and its zeta potentials only positively shifted as compared with that of Mt, demonstrating that a small amount of PEI could not saturate the CEC of Mt and alter its surface charge. On the other hand, the adsorption amount of PHF was still relatively large when the solution pH was above the pH_{zpc} of 10%PEI-Mt, although the electrostatic interaction between PHF and PEI became weak because of the formation of the neutral PEI-Mt composites. Several previous studies disclosed that a great number of amino groups on PEI could generate strong attraction with other organic compounds through hydrogen bonding (Chibowski et al., 2009; Wang et al., 2015). As such, one might propose that the hydrogen bonding between PEI and PHF could contribute to the high adsorption capacity at high pH values.

Table 2
Langmuir and Freundlich equation parameters for the adsorption isotherms of PHF on various adsorbents.

	Langmuir model			Freundlich model		
	Q_m (mg/g)	b (L/mg)	R^2	K_F	n	R^2
Mt	16.42	0.037	0.9962	2.10	0.828	0.8928
2%PEI-Mt	86.21	0.013	0.9941	1.41	1.157	0.9937
10%PEI-Mt	212.77	0.026	0.9986	2.39	5.528	0.9609

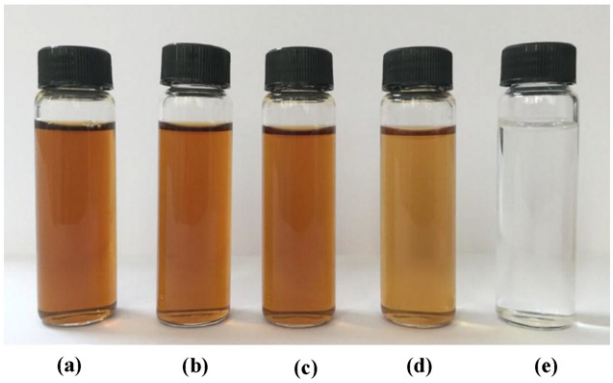

Fig. 3. Visual examination of the PHF solution with the initial concentration of 400 mg/L (a) and the supernatants after the adsorption experiments and centrifugal separation (the adsorbents used were 2%PEI(b), 10%PEI(c), 2%PEI-Mt(d), and 10%PEI-Mt(e), respectively).

The adsorption isotherms were obtained to assess the adsorption capacities of the adsorbents toward PHF (Fig. 2a). The adsorption capacities of PHF on PEI-Mt were much higher than that on Mt. The electrostatic repulsion between the negatively charged Mt and PHF should be the reason for the poor adsorption of PHF on Mt (~16 mg/g). The adsorption amounts may be ascribed to some special interactions, such as hydrogen bonding between PHF and terminal hydroxyl groups of Mt or 'cation-bridging' through the exchangeable cations (Theng, 1982; Fortner et al., 2012). By contrast, PEI-Mt showed strong interaction with PHF, and the maximum adsorption amount of PHF on 10%PEI-Mt could reach ~210 mg/g (Fig. 2b). Combined with the results of zeta potentials above, the protonation of amine groups endowed the surface of 10%PEI-Mt with a number of positive charges under the adsorption experiment condition (pH = 6). Thereby, the electrostatic interaction between the adsorbents and the adsorbates were enhanced.

Langmuir and Freundlich isotherm models were used to quantitatively analyze the adsorption isotherms (Table 2). As shown by the R^2 values, the adsorption isotherms of PHF on three adsorbents were better fitted with the Langmuir model, suggesting the monolayer adsorption on the adsorbents with identical adsorption sites. In light of the calculated Q_m values (Table 2), the adsorption capacities of PHF on the adsorbents increased in the order Mt < 2%PEI-Mt < 10%PEI-Mt.

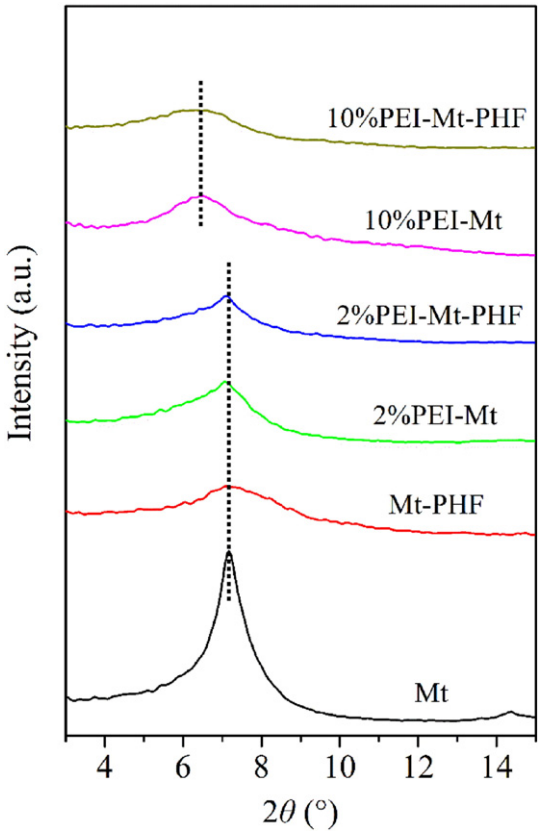

Fig. 5. XRD patterns of Mt, Mt-PHF, 2%PEI-Mt, 2%PEI-Mt-PHF, 10%PEI-Mt, and 10%PEI-Mt-PHF.

As a control experiment, the PHF removal efficiency from aqueous solution by PEI (*i.e.*, in the absence of Mt) was also studied under the same adsorption conditions. As shown by the photographs of the PHF solution and the supernatants after the adsorption experiments, the PHF solution was dark brown (Fig. 3a). The treatment of PHF by PEI hardly changed the color of the supernatants (Fig. 3b and c). In effect, no visible precipitates were obtained after the centrifugal separation

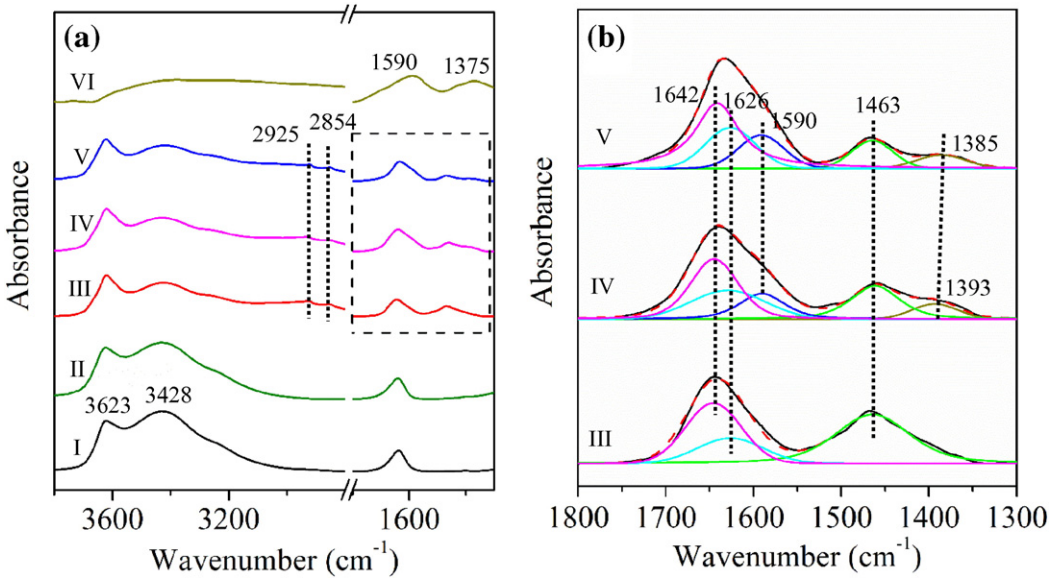

Fig. 4. (a) FTIR spectra of (I) Mt, (II) Mt-PHF, (III) 10%PEI-Mt, (IV) 10%PEI-Mt-PHF (pH = 11), (V) 10%PEI-Mt-PHF (pH = 6), and (VI) PHF; (b) the enlarged views of (III), (IV), and (V) in the range of 1800–1300 cm^{-1}.

of the mixture of PHF and PEI. These results showed that the PEI alone was not effective in removing PHF from water. In contrast, the supernatants became light brown and even completely transparent after the addition of 2%PEI-Mt and 10%PEI-Mt, respectively (Fig. 3d and e). The distinctly different results from the visual examination further manifested that PEI-Mt exhibited outstanding adsorption capacity toward PHF, and can be desirable for the treatment of the PHF wastewater.

The FTIR spectra of the samples were recorded to study the structural changes of the functional groups during the adsorption processes (Fig. 4a). The absorption bands at 3623 and 3428 cm^{-1} on the spectrum of Mt could be assigned to the structural OH and water molecule stretching vibrations, respectively (He et al., 2004, 2006b; Chen et al., 2014). The spectrum hardly altered for Mt after the adsorption of PHF (*i.e.*, Mt-PHF), which may be due to a very small adsorption amount of PHF on Mt. As for PEI-Mt, the intensity of these absorption bands decreased, implying the reduction of their concentration resulting from the diluting effect by the loaded PEI. Moreover, the two absorption bands at ~2925 and 2854 cm^{-1} (arising from the asymmetric and symmetric stretching vibrations of CH_2 groups, respectively) on PEI-Mt further confirmed the presence of PEI (He et al., 2004; Zhu et al., 2008; Zhu et al., 2014). To be clear, the spectrums in the range of 1800–1300 cm^{-1} were decomposed into five components at approximately 1642, 1626, 1590, 1463, and 1385 cm^{-1}, which correspond to OH bending of water, N—H bending, the C═C stretching, CH_2 bending, and C—O—H bending vibrations, respectively (He et al., 2004; Xing et al., 2004; Zhu et al., 2005; Zhang et al., 2009; Hwang and Li, 2010; Ma et al., 2016) (Fig. 4b and Table S1). In comparison with 10%PEI-Mt, the adsorption of PHF caused the decrease of the band intensity at ~1642, ~1626, and ~1463 cm^{-1} and the appearance of the band at ~1590 and ~1385 cm^{-1} in the spectrum of 10%PEI-Mt-PHF. Interestingly, the band at 1375 cm^{-1}, arising from C—O—H bending vibrations, blue-shifted to 1385 and 1393 cm^{-1} for 10%PEI-Mt-PHF obtained at pH 6 and 11, respectively, which suggested strong interaction between the adsorbed PHF and PEI-Mt, probably the formation of hydrogen bonding between them. A similar phenomenon was observed by Wang et al. (2015) who disclosed that the enhanced hydrogen bonding between PEI and anionic compounds at high pH values could lead to a visible shift on the corresponding FTIR band vibrations.

XRD has been regarded as a powerful tool to study the microstructure of clay minerals (He et al., 2005, 2006a, 2010; Vicente et al., 2013; Chen et al., 2016). In the present work, the XRD patterns of the adsorbents before and after the adsorption of PHF were compared (Fig. 5). The sharp diffraction peak attributed to the (001) reflection of Mt indicated a typical Na^+ form with one water layer in the interlayer space of Mt (He et al., 2006c; Vicente et al., 2013). After treatment with 2%PEI, the modified Mt exhibited the same basal spacing with the raw Mt (~1.24 nm). On the other hand, the basal spacing of 10%PEI-Mt slightly increased to 1.47 nm. In this regard, one would expect that PEI should mainly existed on the external surface of 2%PEI-Mt but it could be intercalated into the interlayer space of Mt with rising PEI loading amount. In addition, the adsorption of PHF hardly altered the basal spacing of all the adsorbents. The unchanged basal spacing of Mt further confirmed that PHF were mostly adsorbed at surfaces and edges of Mt through some special interaction. According to the above discussion, the adsorption sites on PEI-Mt should mainly originate from PEI that covered on the external surfaces. Moreover, the large size of a PHF molecule (~1.4 nm) might hinder the utility of the adsorption sites within the interlayer space of PEI-Mt.

The morphologies of the adsorbents with or without adsorbing PHF were investigated by TEM. Semitransparent texture with lamellar structures were observed in the TEM image of Mt (Fig. 6a). PEI-Mt retained the same layered morphology as the pristine Mt (Fig. 6c). As for the TEM image of Mt/PHF (the mixture of Mt and PHF), it exhibited a loose, agglomerate, and uneven morphology (Fig. 6b), indicating that

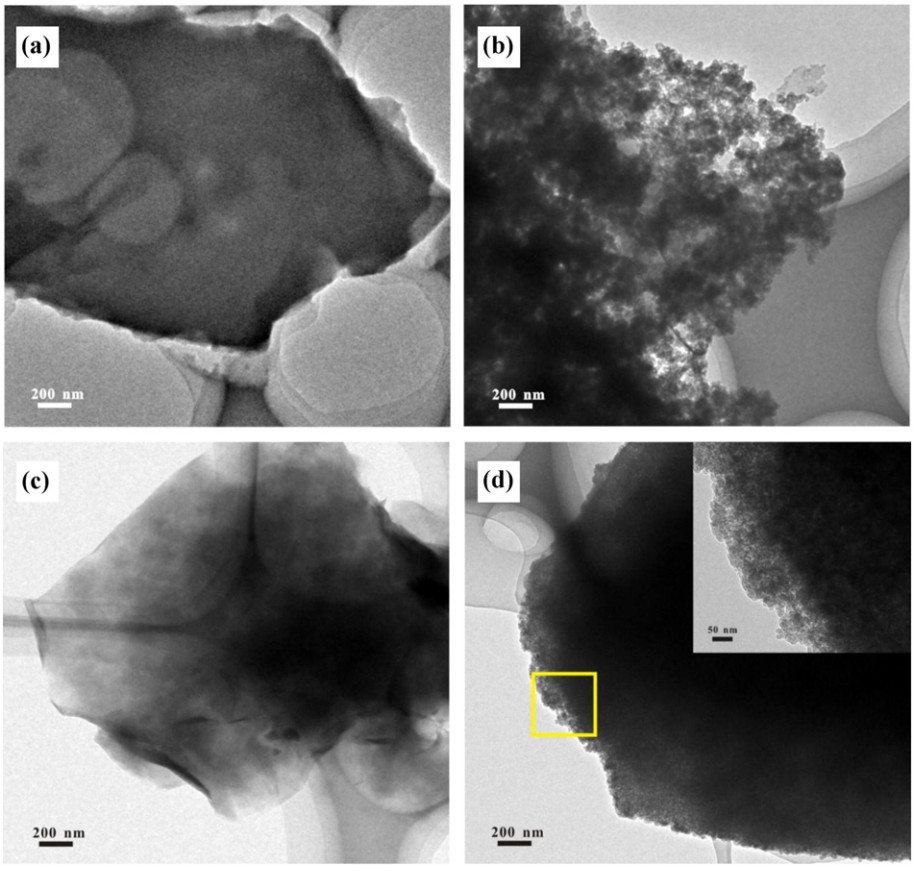

Fig. 6. TEM images of Mt(a), Mt/PHF(b), 10%PEI-Mt(c), and 10%PEI-Mt/PHF(d).

PHF significantly clustered on the surfaces of Mt. The reason might be that the special interactions (*e.g.*, the limited terminal hydroxyl groups and 'cation-bridging') could not provide enough adsorption sites for PHF, so that PHF tended to cluster by itself on the surfaces. Compared to that of Mt/PHF, a uniform morphology was obtained for 10%PEI-Mt/PHF (Fig. 6d), which could be ascribed to the even distribution of the adsorbed PHF on the adsorption sites of the surfaces, *i.e.*, without forming PHF aggregates.

The above results clearly showed that PEI-Mt had favorable adsorption capacities toward PHF and can be used as a low-cost and high-efficient adsorbent in the removal of PHF from aqueous solution. Meanwhile, given that Mt is ubiquitous in soils and sediments and may form various composites with natural organic macromolecules (Bergaya and Lagaly, 2013), the present work may provide novel information for understanding the migration and sequestration of carbon nanomaterials in the environment. In other words, PHF may be well immobilized by natural clay-macromolecules composites.

4. Conclusion

In summary, the modification of Mt with a branched polymer PEI developed a novel adsorbent, PEI-Mt, for the remediation of the wastewater containing PHF. The adsorption experiments demonstrated that PEI-Mt showed superior adsorption capacity for PHF over a wide variety of solution pH range, which could be attributed to the combined contributions of the electrostatic attraction and the hydrogen-bond interaction between PHF and PEI-Mt. The adsorption amounts of PHF on PEI-Mt increased with rising PEI loading amount on Mt and with decreasing solution pH. The adsorption equilibrium data of PHF on all the absorbents were well fitted with the Langmuir model, and the calculated maximum adsorption amount of PHF on 10%PEI-Mt reached ~213 mg/g, much higher than that on the original Mt (~16 mg/g). In addition, the XRD and TEM results revealed that the adsorbed PHF mainly existed on the external surfaces of PEI-Mt. This work indicated that PEI-Mt had high affinity toward PHF and could be applied as a potentially desirable adsorbent for the removal of PHF from aqueous solution.

Acknowledgments

This work was financially supported by the National Natural Science Foundation of China (41322014, 41572031), Guangdong Provincial Youth Top-notch Talent Support Program (2014TQ01Z249), and National Youth Top-notch Talent Support Program, CAS/SAFEA International Partnership Program for Creative Research Teams (20140491534), and Zhejiang Provincial Natural Science Foundation of China (LY16B070005). This is contribution No.IS-2268 from GIGCAS.

Appendix A. Supplementary data

Supplementary data to this article can be found online at http://dx.doi.org/10.1016/j.clay.2016.07.007.

References

Amara, M., Kerdjoudj, H., 2003. Modification of the cation exchange resin properties by impregnation in polyethyleneimine solutions: application to the separation of metallic ions. Talanta 60, 991–1001.
An, H.J., Jin, B., 2012. Impact of fullerene particle interaction on biochemical activities in fermenting *Zymomonas mobilis*. Environ. Toxicol. Chem. 31, 712–716.
Bergaya, F., Lagaly, G., 2013. Chapter 1–General Introduction: Clays, Clay Minerals, and Clay Science. In: Bergaya, F., Lagaly, G. (Eds.), Developments in Clay Science vol. 5 A. Elsevier, pp. 1–19.
Brant, J.A., Labille, J., Bottero, J.-Y., Wiesner, M.R., 2006. Characterizing the impact of preparation method on fullerene cluster structure and chemistry. Langmuir 22, 3878–3885.
Brant, J.A., Labille, J., Robichaud, C.O., Wiesner, M., 2007. Fullerol cluster formation in aqueous solutions: implications for environmental release. J. Colloid Interface Sci. 314, 281–288.
Chae, S.-R., Hunt, D.E., Ikuma, K., Yang, S., Cho, J., Gunsch, C.K., Liu, J., Wiesner, M.R., 2014. Aging of fullerene C_{60} nanoparticle suspensions in the presence of microbes. Water Res. 65, 282–289.
Chen, Q.Z., Zhu, R.L., Deng, W.X., Xu, Y., Zhu, J.X., Tao, Q., He, H.P., 2014. From used montmorillonite to carbon monolayer–montmorillonite nanocomposites. Appl. Clay Sci. 100, 112–117.
Chen, Q.Z., Liu, H.M., Zhu, R.L., Wang, X., Wang, S.Y., Zhu, J.X., He, H.P., 2016. Facile synthesis of nitrogen and sulfur co-doped graphene-like carbon materials using methyl blue/montmorillonite composites. Microporous Mesoporous Mater. 225, 137–143.
Chibowski, S., Patkowski, J., Grządka, E., 2009. Adsorption of polyethyleneimine and polymethacrylic acid onto synthesized hematite. J. Colloid Interface Sci. 329, 1–10.
Colvin, V.L., 2003. The potential environmental impact of engineered nanomaterials. Nat. Biotechnol. 21, 1166–1170.
Fortner, J.D., Solenthaler, C., Hughes, J.B., Puzrin, A.M., Plötze, M., 2012. Interactions of clay minerals and a layered double hydroxide with water stable, nano scale fullerene aggregates (nC_{60}). Appl. Clay Sci. 55, 36–43.
Gao, B.J., Li, Y.B., Chen, Z.P., 2009. Adsorption behaviour of functional grafting particles based on polyethyleneimine for chromate anions. Chem. Eng. J. 150, 337–343.
Georgieva, A.T., Pappu, V., Krishna, V., Georgiev, P.G., Ghiviriga, I., Indeglia, P., Xu, X., Fan, Z.H., Koopman, B., Pardalos, P.M., Moudgil, B., 2013. Polyhydroxy fullerenes. J. Nanopart. Res. 15, 1–18.
He, H.P., Frost, R.L., Zhu, J.X., 2004. Infrared study of $HDTMA^+$ intercalated montmorillonite. Spectrochim. Acta. Part A 60, 2853–2859.
He, H.P., Duchet, J., Galy, J., Gérard, J.-F., 2005. Grafting of swelling clay materials with 3-aminopropyltriethoxysilane. J. Colloid Interface Sci. 288, 171–176.
He, H.P., Duchet, J., Galy, J., Gérard, J.-F., 2006a. Influence of cationic surfactant removal on the thermal stability of organoclays. J. Colloid Interface Sci. 295, 202–208.
He, H.P., Yang, D., Yuan, P., Shen, W., Frost, R.L., 2006b. A novel organoclay with antibacterial activity prepared from montmorillonite and Chlorhexidini Acetas. J. Colloid Interface Sci. 297, 235–243.
He, H.P., Zhou, Q., Martens, W.N., Kloprogge, T.J., Yuan, P., Xi, Y.F., Zhu, J.X., Frost, R.L., 2006c. Microstructure of $HDTMA^+$-modified montmorillonite and its influence on sorption characteristics. Clay Clay Miner. 54, 689–696.
He, H.P., Ma, Y.H., Zhu, J.X., Yuan, P., Qing, Y.H., 2010. Organoclays prepared from montmorillonites with different cation exchange capacity and surfactant configuration. Appl. Clay Sci. 48, 67–72.
Hwang, Y.S., Li, Q.L., 2010. Characterizing photochemical transformation of aqueous nC_{60} under environmentally relevant conditions. Environ. Sci. Technol. 44, 3008–3013.
Kang, Q., Zhou, W.Z., Li, Q., Gao, B.Y., Fan, J.X., Shen, D.Z., 2009. Adsorption of anionic dyes on poly(epicholorohydrin dimethylamine) modified bentonite in single and mixed dye solutions. Appl. Clay Sci. 45, 280–287.
Kiser, M.A., Ryu, H., Jang, H., Hristovski, K., Westerhoff, P., 2010. Biosorption of nanoparticles to heterotrophic wastewater biomass. Water Res. 44, 4105–4114.
Klaine, S.J., Alvarez, P.J., Batley, G.E., Fernandes, T.F., Handy, R.D., Lyon, D.Y., Mahendra, S., McLaughlin, M.J., Lead, J.R., 2008. Nanomaterials in the environment: behavior, fate, bioavailability, and effects. Environ. Toxicol. Chem. 27, 1825–1851.
Kwag, D.S., Park, K., Oh, K.T., Lee, E.S., 2013. Hyaluronated fullerenes with photoluminescent and antitumoral activity. Chem. Commun. 49, 282–284.
Li, M., Li, Y.F., Zhou, Z., Shen, P.W., Chen, Z.F., 2009. Ca-coated boron fullerenes and nanotubes as superior hydrogen storage materials. Nano Lett. 9, 1944–1948.
Li, Q., Su, Y., Yue, Q.-Y., Gao, B.-Y., 2011. Adsorption of acid dyes onto bentonite modified with polycations: kinetics study and process design to minimize the contact time. Appl. Clay Sci. 53, 760–765.
Ma, L.Y., Zhu, J.X., Xi, Y.F., Zhu, R.L., He, H.P., Liang, X.L., Ayoko, G.A., 2015. Simultaneous adsorption of Cd (II) and phosphate on Al_{13} pillared montmorillonite. RSC Adv. 5, 77227–77234.
Ma, L.Y., Chen, Q.Z., Zhu, J.X., Xi, Y.F., He, H.P., Zhu, R.L., Tao, Q., Ayoko, G.A., 2016. Adsorption of phenol and Cu(II) onto cationic and zwitterionic surfactant modified montmorillonite in single and binary systems. Chem. Eng. J. 283, 880–888.
Markovic, Z., Trajkovic, V., 2008. Biomedical potential of the reactive oxygen species generation and quenching by fullerenes (C_{60}). Biomaterials 29, 3561–3573.
Meng, Z.-D., Ghosh, T., Zhu, L., Choi, J.-G., Park, C.-Y., Oh, W.-C., 2012. Synthesis of fullerene modified with Ag_2S with high photocatalytic activity under visible light. J. Mater. Chem. 22, 16127–16135.
Prylutskyy, Y.I., Petrenko, V.I., Ivankov, O.I., Kyzyma, O.A., Bulavin, L.A., Litsis, O.O., Evstigneev, M.P., Cherepanov, V.V., Naumovets, A.G., Ritter, U., 2014. On the origin of C_{60} fullerene solubility in aqueous solution. Langmuir 30, 3967–3970.
Qu, X.L., Hwang, Y.S., Alvarez, P.J.J., Bouchard, D., Li, Q.L., 2010. UV irradiation and humic acid mediate aggregation of aqueous fullerene (nC_{60}) nanoparticles. Environ. Sci. Technol. 44, 7821–7826.
Rather, J.A., De Wael, K., 2013. Fullerene-C_{60} sensor for ultra-high sensitive detection of bisphenol-A and its treatment by green technology. Sensors Actuators B Chem. 176, 110–117.
Roberts, M.G., Li, H., Teppen, B.J., Boyd, S.A., 2006. Sorption of nitroaromatics by ammonium-and organic ammonium-exchanged smectite: shifts from adsorption/complexation to a partition-dominated process. Clay Clay Miner. 54, 426–434.
Sayes, C.M., Fortner, J.D., Guo, W., Lyon, D., Boyd, A.M., Ausman, K.D., Tao, Y.J., Sitharaman, B., Wilson, L.J., Hughes, J.B., West, J.L., Colvin, V.L., 2004. The differential cytotoxicity of water-soluble fullerenes. Nano Lett. 4, 1881–1887.
Tang, F.Q., Huang, X.X., Zhang, Y.F., Guo, J.K., 2000. Effect of dispersants on surface chemical properties of nano-zirconia suspensions. Ceram. Int. 26, 93–97.
Theng, B.K.G., 1982. Clay–polymer interactions: summary and perspectives. Clay Clay Miner. 30 (1982), 1–10.
Vicente, M.A., Gil, A., Bergaya, F., 2013. Chapter 10.5–Pillared Clays and Clay Minerals. In: Bergaya, F., Lagaly, G. (Eds.), Developments in Clay Science vol. 5 A. Elsevier, pp. 523–557.

Wang, C., Dai, J., Shang, C., Chen, G.H., 2013. Removal of aqueous fullerene nC_{60} from wastewater by alum-enhanced primary treatment. Sep. Purif. Technol. 116, 61–66.
Wang, S.M., Li, Z.H., Lu, C., 2015. Polyethyleneimine as a novel desorbent for anionic organic dyes on layered double hydroxide surface. J. Colloid Interface Sci. 458, 315–322.
Wielgus, A.R., Zhao, B.Z., Chignell, C.F., Hu, D.-N., Roberts, J.E., 2010. Phototoxicity and cytotoxicity of fullerol in human retinal pigment epithelial cells. Toxicol. Appl. Pharmacol. 242, 79–90.
Xing, G.M., Zhang, J., Zhao, Y.L., Tang, J., Zhang, B., Gao, X.F., Yuan, H., Qu, L., Cao, W.B., Chai, Z.F., Ibrahim, K., Su, R., 2004. Influences of structural properties on stability of fullerenols. J. Phys. Chem. B 108, 11473–11479.
Xiong, S., Yang, F., Jiang, H., Ma, J., Lu, X.H., 2012. Covalently bonded polyaniline/fullerene hybrids with coral-like morphology for high-performance supercapacitor. Electrochim. Acta 85, 235–242.
Yang, K., Zhu, L.Z., Xing, B.S., 2006. Adsorption of polycyclic aromatic hydrocarbons by carbon nanomaterials. Environ. Sci. Technol. 40, 1855–1861.
Yang, Y.K., Nakada, N., Tanaka, H., 2013. Adsorption of fullerene nC_{60} on activated sludge: kinetics, equilibrium and influencing factors. Chem. Eng. J. 225, 365–371.
Yuan, G.D., Theng, B.K.G., Churchman, G.J., Gates, W.P., 2013. Chapter 5.1–Clays and Clay Minerals for Pollution Control. In: Bergaya, F., Lagaly, G. (Eds.), Developments in Clay Science vol. 5B. Elsevier, pp. 587–644.
Yue, Q.-Y., Li, Q., Gao, B.-Y., Wang, Y., 2007. Kinetics of adsorption of disperse dyes by polyepicholorohydrin-dimethylamine cationic polymer/bentonite. Sep. Purif. Technol. 54, 279–290.
Zhang, X.-Q., Chen, M., Lam, R., Xu, X.Y., Osawa, E., Ho, D., 2009. Polymer-functionalized nanodiamond platforms as vehicles for gene delivery. ACS Nano 3, 2609–2616.
Zhang, S., Kang, P., Ubnoske, S., Brennaman, M.K., Song, N., House, R.L., Glass, J.T., Meyer, T.J., 2014. Polyethylenimine-enhanced electrocatalytic reduction of CO_2 to formate at nitrogen-doped carbon nanomaterials. J. Am. Chem. Soc. 136, 7845–7848.
Zhou, J.B., Wu, P.X., Dang, Z., Zhu, N.W., Li, P., Wu, J.H., Wang, X.D., 2010. Polymeric Fe/Zr pillared montmorillonite for the removal of Cr(VI) from aqueous solutions. Chem. Eng. J. 162, 1035–1044.
Zhu, X.W., Tang, F.Q., Suzuki, T.S., Sakka, Y., 2003. Role of the initial degree of ionization of polyethylenimine in the dispersion of silicon carbide nanoparticles. J. Am. Ceram. Soc. 86, 189–191.
Zhu, J.X., He, H.P., Zhu, L.Z., Wen, X.Y., Deng, F., 2005. Characterization of organic phases in the interlayer of montmorillonite using FTIR and ^{13}C NMR. J. Colloid Interface Sci. 286, 239–244.
Zhu, J.X., Yuan, P., He, H.P., Frost, R.L., Tao, Q., Shen, W., Bostrom, T., 2008. In situ synthesis of surfactant/silane-modified hydrotalcites. J. Colloid Interface Sci. 319, 498–504.
Zhu, R.L., Wang, T., Zhu, J.X., Ge, F., Yuan, P., He, H.P., 2010. Structural and sorptive characteristics of the cetyltrimethylammonium and polyacrylamide modified bentonite. Chem. Eng. J. 160, 220–225.
Zhu, R.L., Chen, W.X., Shapley, T.V., Molinari, M., Ge, F., Parker, S.C., 2011. Sorptive characteristics of organomontmorillonite toward organic compounds: a combined LFERs and molecular dynamics simulation study. Environ. Sci. Technol. 45, 6504–6510.
Zhu, R.L., Chen, Q.Z., Liu, H.Y., Ge, F., Zhu, L.F., Zhu, J.X., He, H.P., 2014. Montmorillonite as a multifunctional adsorbent can simultaneously remove crystal violet, cetyltrimethylammonium, and 2-naphthol from water. Appl. Clay Sci. 88-89, 33–38.
Zhu, R.L., Chen, Q.Z., Zhou, Q., Xi, Y.F., Zhu, J.X., He, H.P., 2016. Adsorbents based on montmorillonite for contaminant removal from water: a review. Appl. Clay Sci. 123, 239–258.